

Research Article

Quantitative Assessment of Skull-Base Invasion in Nasopharyngeal Carcinoma Patients with Signal Intensity Index Based on Magnetic Resonance Imaging

Yi-Zhuo Li¹, Chuan-Miao Xie¹, Yao-Pan Wu¹, Chun-Yan Cui¹, Zi-Lin Huang¹, Ci-Yong Lu², Pei-Hong Wu¹

¹Imaging Diagnosis and Interventional Center, State Key Laboratory of Oncology in Southern China, Cancer Center, Sun Yat-sen University, Collaborative Innovation Center for Cancer Medicine. Guangzhou, People's Republic of China.

²Faculty of Medical Statistics and Epidemiology School of Public Health, Sun Yat-sen University, Guangzhou, Guangdong Province, The People's Republic of China, 510080.

Corresponding author: Prof. Pei-Hong Wu, M.D. Imaging Diagnosis and Minimally Invasive Interventional Center, State Key Laboratory of Oncology in Southern China, Cancer Center, Sun Yat-Sen University, Collaborative Innovation Center for Cancer Medicine. No. 651 Dongfeng Road East, Guangzhou 510060, China. Tel: 86-20-87343272; Fax: 86-20-87343272; E-mail: wupeihong56@126.com.

Citation: Li YZ, Xie CM, Wu YP, Cui CY, Huang ZL, Lu CY, Wu PH. Quantitative Assessment of Skull-Base Invasion in Nasopharyngeal Carcinoma Patients with Signal Intensity Index Based on Magnetic Resonance Imaging[J]. J Nasopharyng Carcinoma, 2015, 2(5): e25.doi:10.15383/jnpc.25.

Competing interests: The authors have declared that no competing interests exist.

Conflict of interest: None

Copyright: ©2015 By the Editorial Department of Journal of Nasopharyngeal Carcinoma. All rights reserved. This is an open-access article distributed under the terms of the Creative Commons Attribution License, which permits unrestricted use, distribution, and reproduction in any medium, provided the original author and source are credited.

Abstract: Purpose: To evaluate the use of signal intensity index (SII) of skull-base invasion in nasopharyngeal carcinoma (NPC) based on magnetic resonance imaging (MRI), and to select the best cut-off SII value to predict the outcome of NPC. **Materials and Methods:** One hundred and twenty-two NPC patients with skull-base invasion were included. All patients underwent MRI, signal intensities on T1-weighted imaging (T1WI) were measured for each invaded site and that of its contralateral normal counterpart. The SIIs were calculated, and receiver operating characteristic curves (ROC) were constructed. The optimal cut-off values were extracted. The overall survival (OS) rates of 5-year follow-up were performed. **Results:** There were three cut-off values for differentiating invasion from normal anatomy of skull-base, 49%, 98%, and 60%. Sensitivities for differentiating skull-base invasion from normal contralateral anatomy were 98.9%, 88.5% and 70.0%, and specificities were 98.9%, 96.0% and 74.4%, respectively. Significant difference in OS rates (84.2% vs. 57.1%, $P=0.007$) was seen

between high SII (>60%) and low ($\leq 60\%$) (84.2% vs. 57.1%, $P = 0.007$). **Conclusions:** The SII might be a useful means to differentiate invasion from normal tissue at the skull-base in NPC. The suggested cut-off value of quantitative SII at the skull-base is 60%, and it may aid in monitoring the response to treatment of NPC patients.

Keywords: Nasopharyngeal carcinoma; magnetic resonance imaging; Skull-base invasion; Signal intensity index; cut-off value

Introduction

Nasopharyngeal carcinoma (NPC) often involves the base of the skull. Skull-base invasion is considered to be one of the unfavorable prognostic factors^[1]. Such tumors that involve the base of the skull are classified as stage T3 under American Joint Committee on Cancer (AJCC)/Union for International Cancer Control (UICC) criteria[2]. However, there are not any literatures on quantitative diagnostic criteria for assessing whether the skull base were invaded or not. Owing to their anatomic location, histopathologic data of skull-base are not readily acquired for confirmation of skull-base invasion. Previous studies have used several visual MR criteria alone to diagnose skull-base invasion, such as the degree to which defects in the low signal intensity of the cortex and marrow have been replaced by tumor, as assessed using contrast enhancement in bone^[3-6]. This definition is ambiguous, not quantitative and does not provide a solid guideline for differentiating between skull-base invasion and normal bone.

The current study focused on the signal intensity response of the skull-base in patients before and after definitive radiation therapy based on MRI. We, therefore, retrospectively evaluated whether the signal intensity index (SII) can be of diagnostic and prognostic value in NPC patients with skull-base invasion based on MRI.

Materials and Methods

Patient Characteristics: The approval of the institutional review board was obtained for this study. All examinations were performed after obtaining written informed consent form from either patients or their next of kin. From January 1, 2003 to March 31, 2005, a total number of 548 patients (412 men, 136 women; median age, 44 years; range, 13–76 years) were diagnosed with skull-base invasion in untreated NPC patients. The diagnosis was based on using Spin Echo T1W MR images, which is a reliable and accurate means of differentiating invaded areas from the normal skull-base in NPC patients. Four hundred and two patients had only invaded with the base of the sphenoid bone by NPC, which is too thin to be measured using a circular or elliptical cursor; six patients failed to complete radiation therapy; and eighteen patients lost during the follow-up. These patients were excluded. Therefore, among the 548 patients, 122 patients (92 men, 30 women; median age, 43 years; age range, 13–76 years) met all the following criteria for inclusion in this study: (a) biopsy-proven NPC not previously treated; (b) MRI scan of the head and neck within 1 week to the start of treatment; (c) at least one measurable skull-base invasion area on T1W MR images without and with the use of intravenous contrast agent; (d) bone involvement on MRI diagnosed via any a defect in the low signal intensity of the cortex and marrow replaced by tumor as visualized with contrast enhancement in bone; (e) during follow-up, the MR images and the clinical data before and after radiation therapy were all available. All

patients were staged using the AJCC/UICC staging system^[2]. World Health Organization (WHO) histological classification of the tumors included type I (two patients), type II (30 patients), and type III tumors (90 patients). Clinical staging consisted of 39 stage III patients and 83 stage IV patients.

Imaging Protocols: All patients underwent MRI using a 1.5-T system (Signa, CV/i, GE Healthcare, Milwaukee, WI, U.S.A.) employing the fast spin-echo technique. The region from the suprasellar cistern to the inferior margin of the sternal end of the clavicle was examined with a combined head and neck coil. T1-weighted images in the axial, coronal, and sagittal planes (repetition time (TR) ms/echo time (TE) ms, 500–600/10–20, 2 excitations, a 22-cm field of view and a 256×512 frequency matrix); and T2-weighted images in the axial plane (4000–6000/95–110, 1 excitation, a 22-cm field of view, and a 256×512 matrix) were obtained before injection of contrast material. After intravenous gadopentetate dimeglumine (Magnevist, Schering, Berlin, Germany) at a dose of 0.1 mmol per kilogram of body weight, T1-weighted axial and sagittal sequences, and T1-weighted fat saturation coronal images were acquired sequentially using parameters similar to those used without gadopentetate dimeglumine. The slice thicknesses were 5mm and the intersection gaps were 1 mm.

Image Assessment: Two radiologists (Y.Z.L, C.M.X., each with over 10 years of experience in NPC MR imaging, at the time of the study) separately evaluated the MR images and measured signal intensity in both, the abnormal areas and the normal contralateral region on T1WI pre-contrast and contrast images. The measurement was performed with electronic calipers in the GE Healthcare Centricity Radiology RA600 (GE Healthcare, Milwaukee, Wis). Any disagreements of the presence or absence of skull base invasion on visual MR images were resolved by consensus. A round or

elliptical region of interest (ROI) cursor was placed over the center of suspicious invasion area and the normal contralateral region. The area of the ROI was 2.40–15.20 mm^[2]. The signal intensity of the normal contralateral region was considered appropriate for use as a reference point for signal intensity. The signal intensity of the invasion was compared to this reference. In each patient, the area, location, and size of the ROI were kept constant between the non-contrast and contrast images, both, before and after radiotherapy. There are 277 areas of bone were measured. (Clivus: 98, Petrousapex: 89, pterygoid process: 90).

The mean signal intensity values and the SII were calculated. The SII was calculated as follows: (a) $ESII = (ESIC - ESIN) / ESIN \times 100$, where ESII is the SII of the skull-base invasion, ESIC is the signal intensity of the invasion area on contrast-enhanced T1W images, and ESIN is the signal intensity of invasion area on non-contrast T1W images; (b) $NSII = (NSIC - NSIN) / NSIN \times 100$, where NSII is the SII of the contralateral normal area, NSIC is the signal intensity of the normal area on contrast enhanced T1W images, and NSIN is the signal intensity of the normal area on non-contrast T1W images. The SIIs was classified to group 1 to 3, consist of the same patients with different terms of follow-up, in untreated patients, in treated patients 3–6 months and over 6 months after radiotherapy, respectively.

Follow-up: All patients were followed regularly with imaging studies and clinical evaluation. The follow-up duration was calculated from the first day of treatment until the date of death or the date of the last MRI study or physical examination, whichever comes first^[7–8]. During the first 2 years of follow-up, the patients were examined every 3 months and thereafter, every 5 months. The untreated patients were designated group 1. Patients who underwent MRI 3–6 months post treatment were classified as group 2. Patients

who underwent MRI over 6 months post treatment were classified as group 3. The median follow-up period for the whole group was 72 months (range, 24–96 months).

Statistical Analysis: All statistical comparisons between the invasion and normal areas in each group were performed using the Statistical Package for the Social Sciences (SPSS, version 16.0, Chicago, IL, U.S.). The criterion for statistical significance was set at $P < 0.05$. To evaluate the diagnostic performance of SII in differentiating skull-base invasion from normal bone, receiver operating characteristic (ROC, Medcalc Software Version 11.6, Belgium) curve analysis was performed. From this analysis, the optimal cut-off values, which showed the best separation (minimal false-negative and false positive results) between the invasion and normal area of skull-base were extracted. Kaplan-Meier curves^[9] were used to quantify the values of the 5-year overall survival (OS) over time. The log-rank test was used to compare the survival rates.

Results

Signal Intensity Indexes: The SIIs in the abnormal and normal contralateral regions in each group are listed in Table 1. Each of the SII was provided numbers 1–6 in a serial-wise manner as indicated in Table 1.

The intensity indexes were significantly different ($P < 0.001$) for the invaded and normal areas.

Table 1. Compare Signal intensity index in normal and invaded areas*.

Group	Normal area (%)	Invaded area (%)	P-value
Group 1	13 ± 3 (In1)	150 ± 40 (In2)	<0.001
Group 2	14 ± 3 (In3)	116 ± 20 (In4)	<0.001
Group 3	8 ± 2 (In5)	29 ± 7 (In6)	<0.001

*:The SIIs of the same patients in untreated, treated in 3–6 months and over 6 months after radiotherapy, was classified to group 1 to 3, respectively. In: signal intensity index.

ROC Analysis in Comparing Normal and Invaded Areas: Based on

the intensity index in the invaded and normal areas in each group, we constructed three ROC curves (Figure 1).

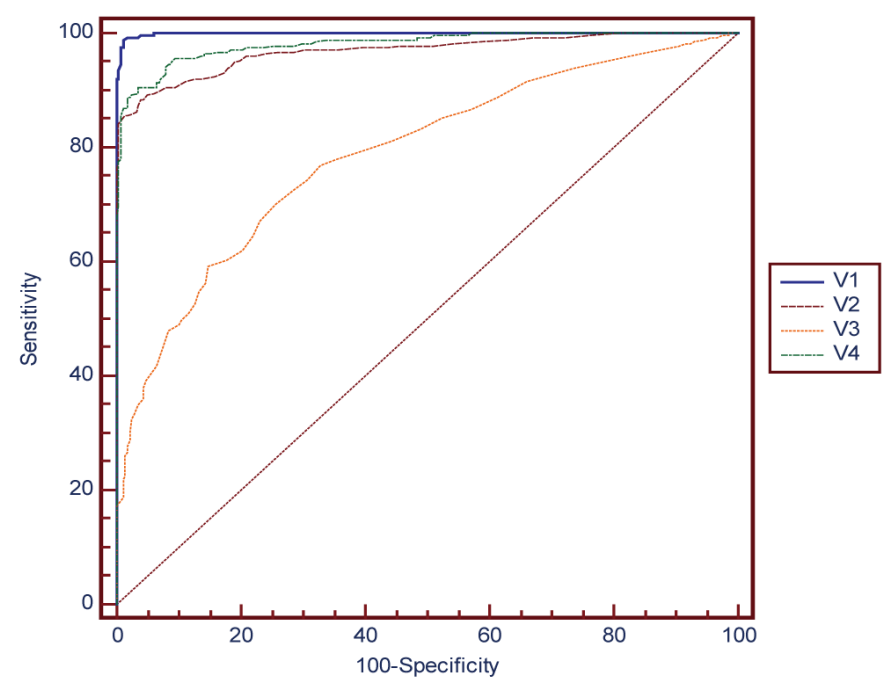


Figure 1: ROC curves of the signal intensity index. V1: In1 versus In2, V2: In3 versus In4, V3: In5 versus In6, V4: In6 versus In2.

V1, V2, and V3 represented the SIIs comparison between the normal and invaded region of groups 1, 2, and 3, respectively, along with an additional ROC curve, V4. In untreated patients (V1), the accuracy of the SII was 99.9% with sensitivity, specificity, and positive and negative predictive values of 98.9%, 98.8%, 98.9%, and 98.9%, respectively (Table 2).

Table 2. The cut-off point, Sensitivity, Specificity, PPV, NPV value of the ROC curves

Criterion	SN	95% CI	SP	95% CI	PPV	95% CI	NPV	95% CI
V1>49	98.92	96.9–99.8	98.92	96.9–99.8	98.9	96.9–99.8	98.9	96.9–99.8
V2>41	88.45	84.1–92.0	96.03	93.0–98.0	95.7	92.4–97.8	89.3	85.2–92.5
V3>13	70.04	64.3–75.4	74.37	68.8–79.4	73.2	67.4–78.4	71.3	65.7–76.4
V4<=53	88.81	84.5–92.3	98.19	95.8–99.4	98.0	95.4–99.4	89.8	85.8–92.0

SN: Sensitivity; SP: Specificity; CI: Confidence Interval; PPV: Positive Predictive Value; NPV: Negative Predictive Value

On follow-up MRI at 3–6 months post-treatment (V2), the accuracy of the SII was 96.9%; and the sensitivity, specificity, and positive and negative predictive values were 88.5%, 96.0%, 95.7%, and 89.3%, respectively. At over 6 months post-treatment, the accuracy of the SII was 78.8%; and the sensitivity, specificity, and positive and negative predictive values were 70.0%, 74.4%, 73.2%, and 71.3%, respectively. The results showed that the efficacy of V3 is

not as strong as that of V1 or V2, and we assumed that this was probably because, in group 3, the tumors had completely resolved. To demonstrate this point of view, we constructed an additional ROC curve, V4, based on the intensity indexes of the eroded areas in group 3 and compared it to those of group 1. The accuracy of the SII was 98.1%; and the sensitivity, specificity, and positive and negative predictive values were 88.8%, 98.2%, 98.0%, and 89.8%, respectively. Among these 4 ROC curves, the ROC before treatment predicted most the erosion because of its highest areas under curve.

Cut-off Value for Differentiating the Treatment Response of Skull

Base Invasion: The SIIs in the abnormal regions among the 3 groups are not the same (Table 1). To evaluate the complete response to treatment, we had a set of comparisons between the SIIs of invaded region of each group and the normal region of group 1 (Table 3).

Table 3. The cut-off, Sensitivity, Specificity between each invaded SIIs and the non-invaded SIIs

zCriterion	SN	95%CI	SP	95%CI	PPV	95%CI	NPV	95%CI
>49 (D1)	98.92	96.9–99.8	98.85	96.7–99.8	98.9	96.9–99.8	98.9	96.7–99.8
≤98 (D2)	47.29	41.3–53.4	80.22	75.0–84.7	70.4	63.3–76.9	60.4	55.2–65.5
≤60 (D3)	90.44	86.3–93.7	96.40	93.5–98.3	96.1	92.9–98.1	91.2	87.3–94.1

CI: Confidence Interval; SN: Sensitivity; SP: Specificity; CI: Confidence Interval; PPV: Positive Predictive Value; NPV: Negative Predictive Value. D1, representing the comparison between the SIIs of invaded region in group 1 (In2) and that of normal region in group 1 (In 1); D2, representing the comparison between the SIIs of invaded region in group 1 (In 2) and that of the invaded region in group 2 (In 4); D3, representing the comparison between the SIIs of invaded region in group 1(In 2) and that of invaded region in group3 (In6).

D1, representing the comparison between the SIIs of invaded region in group 1 (In2) and that of normal region in group 1 (In 1);

D2, representing the comparison between the SIIs of invaded region in group 1 (In 2) and that of the invaded region in group 2

(In 4); D3, representing the comparison between the SIIs of

invaded region in group 1 (In 2) and that of invaded region in group 3 (In6).

In Table 3, the results displayed, that, the optimal cut-off values for differentiating invaded from normal areas in group 1 (D1), was 49%. With this cutoff, the sensitivity, specificity, and positive and negative predictive values were 98.9%, 98.9%, 98.9%, and 98.9%, respectively. The optimal cut-off values for differentiating invaded region between group 1 and group 2 (D2), before treatment versus 3–6 months post treatment) was 98% (the sensitivity, specificity, and positive and negative predictive values were 47.3%, 80.2%, 70.4%, and 60.4%, respectively). The optimal cut-off values for differentiating invaded region between group 1 and group 3 (D3), before treatment versus ≥6 months post treatment) was 60% (the sensitivity, specificity, and positive and negative predictive values were 90.4%, 96.4%, 96.1% and 91.2%, respectively).

Survival Outcomes Correlated with the Cutoff: According to the cut-off of 60% between the SIIs of invaded region in group 1 and group 3, there were 101 patients which SIIs was ≤60% (marked SII subgroup 1) and 21 cases were over 60% (marked SII subgroup 2) in the invaded area over 6-months after treatment. Among subgroup 1, sixteen patients died during clinical follow-up; while in subgroup 2, nine patients died. Significant difference was observed in 5-year OS rates between these two subgroups (84.2% vs. 57.1%, $P=0.007$) (Figure 2).

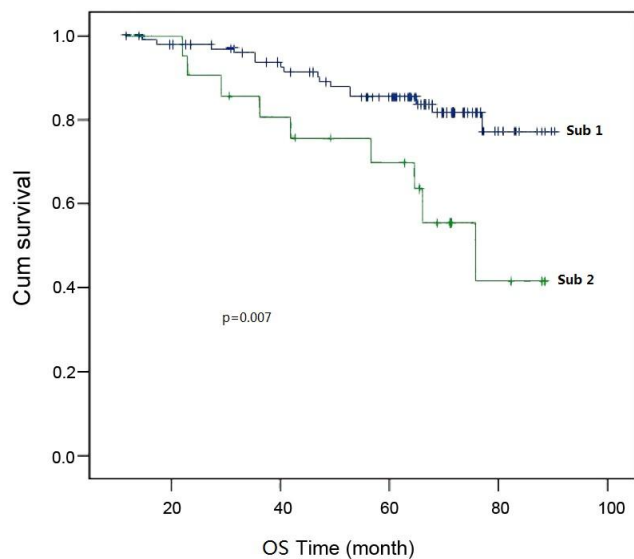


Figure 2: The overall survival (OS) curves for two subgroups of over 6 months post treatment, subgroup 1, SII ≤ 60 ; subgroup 2, SII > 60 .

Discussion

Studies had suggested that F fluorodeoxyglucose (FDG)-positron emission tomography (PET) might be more accurate than MRI in detecting residual/recurrent NPC^[10-13]. However, in a series of 63 patients, Comoretto *et al.*^[14] found that MRI provided more information in assessing skull-base and intracranial lesions, and might facilitate differentiation between mature fibrosis and residual disease. It has also been reported that F-FDG PET/CT might underestimate the presence or extent of tumor invasion in the parapharyngeal space, skull-base, intracranial area, sphenoid sinus and retropharyngeal nodes compared with MRI^[15-16].

In present study we have determined that the quantification of SIIs using Fast Spin Echo T1W MRI is a useful means to differentiate invaded areas from the normal skull-base in NPC patients. The efficacy related parameters at over 6 months after treatment were not as favorable as those of the other groups. This was probably attributed to tumor resolution following radiation therapy in this group. This possibility was demonstrated by the 4th curve in Figure 1. This curve was constructed based on the SIIs in the eroded area of the untreated group versus that of the follow-up MRI over 6 months after treatment. Based on the intensity differences in the three groups, we had set a threshold value that could best discriminate normal from areas with

tumor invasion. A value of $>49\%$ was set for untreated patients, $>98\%$ for the follow-up MRI 3–6 months post treatment, and $>60\%$ for the over 6-month post treatment follow-up MRI. We found (a) when the SIIs of the suspicious invasion area was over 49% in the untreated patients, tumor invasion was present. (b) For radiotherapy-treated patients, when the SII of the suspicious invasion area was 60% or below, a complete resolution was suggested. Our study also showed that the 5-year follow-up OS rate of patients with SII values in the eroded area at 60% or below to be significantly higher than that of over 60%. This result demonstrates that the SII value of 60% may be a reasonable cutoff to mean skull invasion response to therapy. This result may help evaluate and monitor bone tumor response to treatment. In follow up of radiation, a SII of the suspicious eroded area of 60% or less indicated complete tumor resolution; values over 60% but less than 98% indicated partial tumor resolution; and values over 98% indicated no response to treatment. It is worthy to mention that the complete resolution cut-off was $\leq 60\%$, which is different to the $<49\%$ cut-off for untreated patients. Normal tissue response to radiation could be the reason, which was probably the result of the effects of radiation on the dose-limiting organs adjacent to the nasopharynx. The possible difference in biological properties between NPCs with high ($>60\%$ SII) and those with low ($\leq 60\%$ SII) enhancement ratio should be discussed in subsequent study. An initial decrease in SII down to $\leq 60\%$ followed by an increase was taken to indicate tumor recurrence. When the SII increased over 60% but not over 98%, we suspected tumor recurrence, and increases over 98% were taken as indicative of recurrence.

As we all know NPC is treated primarily with radiation therapy, and pathological samples are not available. Thus this study too was not able to correlate to histopathological results. The current study has

other limitations such as its retrospective nature. MRI was chosen to detect skull-base invasion, and probably a comparison with CT would have further complemented the diagnosis of skull-base invasion. The partial volume averaging artifact is a common problem in studies that use ROI measurements. Some anatomical structures, such as the base of the sphenoid bone, are too thin to be measured using a circular or elliptical cursor. Different areas of the skull base may show various SII, but we calculated them with one group of data. In this paper, SII were only used for predicting outcomes. Other factors such as EBV DNA level, tumor volumes could be related to outcome. These drawbacks must be taken into account. We recommend that the quantitative radiological criteria that we propose in this paper should be verified in subsequent studies.

In conclusion, the quantitative signal intensity index of Spin Echo T1WI might be useful in differentiating invasion areas from the normal anatomy of the skull base in NPC patients. In untreated patients, the cut-off value was 49%. Post-treatment, the cut-off value was 60%. The cut-off value of quantitative SIIs at the skull-base may aid in monitoring the response to treatment of NPC patients.

Acknowledgements

We thank our colleagues in the department of medical records, who provided the follow-up data.

References

[1] Heng DM, Wee J, Fong KW, et al. Prognostic factors in 677 patients in Singapore with nondisseminated nasopharyngeal carcinoma[J]. *Cancer*, 1999, 86(10): 1912–1920.

[2] Edge SB, Compton CC. The American Joint Committee on Cancer: the 7th edition of the AJCC cancer staging manual and the future of TNM[J]. *Ann Surg Oncol*, 2010, 17(6): 1471–1474.

[3] Chong VF, Fan YF. Skull base erosion in nasopharyngeal carcinoma: detection by CT and MRI[J]. *Clin Radiol*, 1996, 51(9): 625–631.

[4] Lu JC, Wei Q, Zhang YQ, et al. Influence of MRI abnormality in skull base bone on prognosis of nasopharyngeal carcinoma[J]. *Cancer Radiother*, 2004, 8(4): 230–233.

[5] Li YZ, Wu PH, Huang ZL, et al. Distributions of primary nasopharyngeal carcinoma tumor and patterns of skull base erosion detected by magnetic resonance imaging[J]. *Zhonghua Yi Xue Za Zhi*, 2010, 90(47): 3347–3350.

[6] Chen L, Liu LZ, Mao YP, et al. Grading of MRI-detected skull-base invasion in nasopharyngeal carcinoma and its prognostic value[J]. *Head Neck*, 2011, 33(9): 1309–1314.

[7] Li YZ, Cai PQ, Xie CM, et al. Nasopharyngeal cancer: impact of skull base invasion on patients prognosis and its potential implications on TNM staging[J]. *Eur J Radiol*, 2013, 82(3): e107–e111.

[8] Li YZ, Xie CM, Wu YP, et al. Nasopharyngeal carcinoma patients with retropharyngeal lymph node metastases: a minimum axial diameter of 6 mm is a more accurate prognostic predictor than 5 mm[J]. *AJR Am J Roentgenol*, 2015, 204(1): 20–23.

[9] Kaplan EL, Meier P. Nonparametric estimation from incomplete observations[J]. *Journal of the American statistical association*, 1958, 53(282): 457–481.

[10] Chan SC, Ng SH, Chang JT, et al. Advantages and pitfalls of ¹⁸F-fluoro-2-deoxy-D-glucose positron emission tomography in detecting locally residual or recurrent nasopharyngeal carcinoma: comparison with magnetic resonance imaging[J]. *Eur J Nucl*

- Med Mol Imaging, 2006, 33(9): 1032–1040.
- [11]Liu T, Xu W, Yan WL, et al. FDG-PET, CT, MRI for diagnosis of local residual or recurrent nasopharyngeal carcinoma, which one is the best? A systematic review[J]. Radiother Oncol, 2007, 85(3): 327–335.
- [12]Yen RF, Hung RL, Pan MH, et al. 18-fluoro-2-deoxyglucose positron emission tomography in detecting residual/recurrent nasopharyngeal carcinomas and comparison with magnetic resonance imaging[J]. Cancer, 2003, 98(2): 283–287.
- [13]Chang J, Chan S, Yen T, et al. 2399 : Differential Roles of 18F-FDG PET in Patients With Locoregionally Advanced Nasopharyngeal Carcinoma After Primary Curative Therapy: Response Evaluation and Impact on Management[J]. J Nucl Med, 2006, 47(9):1447–1454.
- [14]Comoretto M, Balestreri L, Borsatti E, et al. Detection and restaging of residual and/or recurrent nasopharyngeal carcinoma after chemotherapy and radiation therapy: comparison of MR imaging and FDG PET/CT[J]. Radiology, 2008, 249(1): 203–211.
- [15]Ng SH, Chan SC, Yen TC, et al. Staging of untreated nasopharyngeal carcinoma with PET/CT: comparison with conventional imaging work-up[J]. Eur J Nucl Med Mol Imaging, 2009, 36(1): 12–22.
- [16]King AD, Ma BB, Yau YY, et al. The impact of 18F-FDG PET/CT on assessment of nasopharyngeal carcinoma at diagnosis[J]. Br J Radiol, 2008, 81(964): 291–298.